Computer Standards & Interfaces 53 (2017) 48–58

Contents lists available at ScienceDirect

Computer Standards & Interfaces

journal homepage: www.elsevier.com/locate/csi

Capacity and spectrum-aware communication framework for wireless sensor network-based smart grid applications

Muhammad Faheem*, Vehbi Cagri Gungor

Department of Computer Engineering, Abdullah Gül University, Kayseri 38039, Turkey

ARTICLE INFO

Keywords:
Smart grid
Wireless sensor network
Fish bone routing
Cognitive radio
Multi-channel

ABSTRACT

Recently, wireless sensor networks (WSNs) have been widely recognized as a promising technology for enhancing various aspects of smart grid and realizing the vision of next-generation electric power system in a cost- effective and efficient manner. However, recent field tests show that wireless links in smart grid environments have higher packet error rates and variable link capacity because of dynamic topology changes, obstructions, electromagnetic interference, equipment noise, multipath effects, and fading. To overcome these communication challenges, in this paper, we propose a data capacity-aware channel assignment (DCA) and fish bone routing (FBR) algorithm for WSN-based smart grid applications. The proposed DCA framework deals with the channel scarcities by dynamically switching between different spectrum bands and employs a network for organizing WSN into a highly stable connected hierarchy. In addition, the proposed FBR mechanism provides robust loop free data paths and avoids high transmission cost, excessive end-to-end delay and restricts unnecessary multi-hop data transmission from the source to destination in the network. Thus, it significantly reduces the probability of data packet loss and preserves stable link qualities among sensor nodes for load balancing and prolonging the lifetime of wireless sensor networks in harsh smart grid environments. Comparative performance evaluations show that our proposed schemes outperform the existing communication architectures in terms of data packet delivery, communication delay and energy consumption.

1. Introduction

The smart grid (SG) is the next-generation power system where power distribution and management is upgraded by employing advanced bi-directional communications, pervasive computing and sensing to significantly improve the agility, efficiency and reliability of the power grid [1]. It offers a way to maintain real-time awareness of operating requirements and capabilities for the electricity providers, distributors and consumers. To this end, an integrated high performance, reliable, scalable and robust communication architecture plays a crucial role to collect timely information from different areas of the grid [2–6]. For the last few years a steep growth has been observed in wireless sensor networks (WSNs) for monitoring applications in various scientific and engineering domains [7–13]. Recently, WSNs have been widely recognized as a promising technology for enhancing various aspects of electric power grid and realizing the vision of next-generation electric power system in a cost-effective and efficient manner. However, the design of WSNs-based reliable communications networks for smart grid has considerable unique challenges, including multipath fading, extremely high attenuation and excessive interference due to nonlinear electric power equipment. This brings several dramatic challenges to static channel, which result in high data packet loss for WSNs-based SG applications [14]. In smart grid, diverse WSN-based SG applications have diverse QoS requirements as shown in Table 1.

Due to late recognition of smart grids, the studies about smart grid communication protocols are found to be limited. Though quality-of-service (QoS) aware routing protocols [15–22] for smart grid exist, but their foci are limited to certain applications, such as price signaling and emergency handling. The majority of these existing solutions have been designed to meet application-specific design objectives and requirements in a particular scenario. Although these studies provide valuable insights and guide design decisions for WSN-based smart grid applications, most of the existing routing schemes achieve one or two of these design objectives at the expense of others. For example, energy saving during data collection introduces excessive delay in the network. Moreover, they generally ignore the impact of external interference and noise on transmission reliability in harsh SG environments. Furthermore, they do not have the ability of channel adaptation to alleviate the interference induced at a certain channel due to the power

* Corresponding author.
E-mail addresses: muhammad.faheem@agu.edu.tr (M. Faheem), cagri.gungor@agu.edu.tr (V. Cagri Gungor).

http://dx.doi.org/10.1016/j.csi.2017.03.003
Received 4 November 2016; Received in revised form 6 March 2017; Accepted 7 March 2017
Available online 15 March 2017

Table 1
QoS requirements of WSN-based smart grid applications [1].

Applications	Bandwidth	Reliability	Latency
Price signalling	9.6–56 kbit/s	99%	2000 ms
Automated feeder switching	9.6–56 kbit/s	99%	1000–2000 ms
Home energy management	9.6–56 kbit/s	99.0–99.99%	300–2000 ms
Distribution Management (DM)	9.6–100 kbit/s	99.0–99.99%	100 ms to 2 s
Smart metering infrastructure	10–100 kbit/s per node, 500 kbit/s for backhaul	99.0–99.99%	2000 ms
Overhead transmission line monitoring	9.6–64 kbit/s	90%	1000 ms
Demand Response	14–100 kbit/s per node	99%	500-ms several minutes
Outage Management	56 kbit/s	99.0%	2000 ms
Residual energy management	9.6–56 kbit/s	99%	1000 ms
Asset Management	56 kbit/s	99.0%	2000 ms
Vehicle to Grid (VG)	9.6-56 kbps	99.0–99.99%	2sc-5 min

grid equipment. Recently, cognitive radio sensor networks (CRSNs) have been proposed to serve as a reliable, robust and efficient data aware communications infrastructure that can address both the existing and future energy management requirements of the SG [23]. However, the routing in CRSNs in the context of collision free cooperative spectrum sensing is still an important problem for SG applications, yielding bursty traffic depending on the event characteristics. Recent field tests show that the time varying nature of the smart grid environment due to the variations of spectrum availabilities needs frequent re-channel assignment [24]. However, the existing network solutions due to their fixed or inefficient channel allocation strategies fail to handle dynamic spectrum access challenges and thus, they are not resilient or efficient enough to provide desired reliable data delivery for WSN-based smart grid applications.

To overcome these communication challenges, in this paper we have three major contributions: First, we propose a data capacity-aware channel assignment (DCA) mechanism. The proposed DCA framework deals with the channel scarcities by dynamically switching between different spectrum bands and employs a network for organizing WSN into a highly stable connected hierarchy. Second, we propose a fish bone routing (FBR) algorithm for WSN-based smart grid applications. The proposed FBR mechanism provides robust loop free data paths and avoids high transmission cost, excessive end-to-end delay and restricts unnecessary multi-hop data transmission from the source to destination in the network. Thus, it significantly reduces the probability of data packet loss and preserves stable link qualities among sensor nodes for load balancing and prolonging the lifetime of wireless sensor networks in harsh smart grid environments. Third, we conducted statistical and experimental simulation studies. Comparative performance evaluations show that our proposed schemes outperform the existing communication architectures in terms of data packet delivery, network reliability, communication delay, and energy consumption for real and high data rate, e.g., automated demand supply, and certain data rate and reliability, e.g., smart metering applications.

The organization of this paper is as follows. Section 2 presents the network model and our proposed data capacity-aware cooperative channel assignment and routing scheme (called CAFBR). The path loss model is presented in Section 3. The simulation model and comparative performance evaluations are discussed in Section 4. Finally, Section 5 concludes the paper.

2. Data capacity-aware spectrum access in fish bone routing (CAFBR)

2.1. Network model

The current and envisioned applications of WSNs in smart grid span a wide range, including substation automation, overhead transmission line monitoring, energy management, advanced metering infrastructure, outage management, distribution automation, demand response and dynamic pricing, load control and energy [11]. In this study, we consider a scenario in which multiple sensor nodes have been deployed in a 500 kV outdoor substation environment and each deployed sensor node is equipped with a single radio transceiver that can be tuned to any channel opportunistically in the licensed spectrum. It is also assumed that all the sensor nodes and sink in the network are deployed in an ad-hoc manner. Second, there are φ_n number of channels which are equal to the stationary primary users φ_{pu} transmitters with their known location and the maximum coverage range φ_r meters. Third, there exist $\varphi_{su(k)}$ secondary users which can occupy channel φ_{ci} from φ_{cn} opportunistically when $\varphi_{pu(n)}$ goes silent for t_{off} seconds. Forth, each geographically distributed sensor node is equal in terms of initial energy. Fifth, during the deployment phase, we assumed omnidirectional communication model, i.e., 360^o. Sixth, to avoid collision we assumed Carrier Sense Multiple Access (CSMA) mechanism. In addition, it is assumed that sensor nodes only can communicate with each other's if they are in the range and have the capability to reconfigure the transmission power. Finally, we assumed that the network includes asymmetric links.

2.2. Data capacity-aware cooperative channel assignment algorithm (DCA)

In CRSNs, secondary users (SUs) sense the temporal absence of primary users (PUs) if occupied then most likely secondary user (SU) will find this channel to be busy. The SU has to give up the sensed channel and switch to another channel and immediately transmit on the identified spectrum holes in CRSNs. Generally, in CRSNs spectrum sensing methods are categorized into cooperative and a non-cooperative approaches to find vacant spectrum bands. In cooperative approach, secondary users perform spectrum sensing and forward the measurements to the central fusion specialized device that fuses the spectrum results and makes decision on the use of spectrum [25]. On the other hand, secondary user makes local decision based on its own spectrum measurement in non-cooperative algorithm approach. It can be envisioned that cooperative spectrum sensing can significantly increases the systems aptitude in recognizing and avoiding primary users. However, a central controller specialized device probable also increase the overall network deployment cost in centralized cooperative algorithm approach. Moreover, it may also require large information exchange overhead, which would not be practical for low cost energy efficiency requirements for CRSNs. Additionally, failure of a single expert device could lead to a particular region cut off and spectrum management problems in large scale smart grid deployment.

To overcome these drawbacks, it is often necessary to make autonomous sensing decisions without the coordination of a central controller. To this end, a decentralized cooperative algorithm approach seems to be the best choice due to its flexibility in deployment. In this approach, a group of secondary users perform spectrum sensing by collaboration where each node locally maintains its channel information and makes decision by itself. However, SUs' sensing capabilities

due to software-defined radio and hardware limitations are usually limited in decentralized cooperative approach.

Although, SUs sequentially sense the whole vacant channels may increase the probability of finding a vacant channel. However, the risk of data packet collision and high interference also increases which may affect the neighboring nodes leading to poor link qualities pretentious by higher interference. Thus, it wastes transmission time and also degrading SUs throughput and delay. To avoid risks SUs could be restricted to a specific region instead of sensing the whole vacant channels. This would be more efficient in terms of interference, sensing delay, sensing overhead and higher transmission efficiency. Moreover, it will also allow multiple SUs to sense different channels simultaneously at extremely low complexity in the network in different regions.

To address challenges, in this study, we consider a decentralized cooperative algorithm approach with restricted spectrum sensing for WSN-based smart grid applications. In smart grid, due to the harsh nature of the deployment environment, variable link quality is considered as the most important challenging issue for the efficient and reliable data transmission. The designed scheme provides a better communication environment to its SUs by replacing the poor quality channel immediately with the environment compatible one. It manages the control tasks for efficient data collection or sensing in an appropriate way to support a wide range of WSN-based smart grid applications. In designed scheme based on prior history desired data capacity channels are assigned to SUs with higher stability, corresponding to longer idle probability. This longer idle probability reduces the collisions occurring between PUs and SUs and saves a significant amount of retransmission power, which is consumed during re-sensing the spectrum holes. In case that desired capacity channel is not found locally then a SU sends its request to its one hop neighboring nodes. The more channels are searched in neighborhood, the higher the likelihood to find a better data capacity channel for supporting the desired QoS requirements. In our scheme, we assume that there are φ_n number of channels which are equal to the stationary primary users φ_{pu} transmitters with their know location and the maximum coverage range φ_r meters.

Let $\sum_{\varphi_{cn}}\{\varphi_{c1}, \varphi_{c2}, \ldots, \varphi_{cn}\}$ denote the channels set and $\sum_{\varphi_{pu}}\{\varphi_{pu1}, \varphi_{pu2}, \ldots, \varphi_{pun}\}$ denote the set of primary users while the set of secondary users can be denoted as $\sum_{\varphi_{su}}\{\varphi_{su1}, \varphi_{su2}, \ldots, \varphi_{sun}\}$. The channel selection problem is that secondary user $\varphi_{su(i)}$ can occupy suitable channel $\varphi_{c(i)}$ from the available channel list $\varphi_{c(n)}$ opportunistically to maximize the total channel utility when $\varphi_{pu\ (i)}$ goes silent for t_{off} seconds. We indicate the activity of secondary users $\varphi_{su(n)}$ in region $\varphi_{r(i)}$ at time $\varphi_{t(i)}$ by a vector $r^{\varphi_{su(n)}T}(\varphi_{t(i)})$, where $r^{\varphi_{su(n)}T} = \{r_1^{\varphi_{su(n)}T}, r_2^{\varphi_{su(n)}T}, \ldots, r_{\varphi_{su(n)}}^{\varphi_{su(n)}T}\}$ and $r^{\varphi_{su(i)}T}(\varphi_{t(i)})$ is the sensing event count of secondary user $\varphi_{su(i)}$ in the time interval $[(n-1)\delta t, n\delta t]$. The sensing event is characterized by its location information φ_l, data capacity (φ_{dc}), noise (φ_{n0}), and interference (φ_i) collectively denoted as $\varphi_i = \{\varphi_{ni}(\varphi_{t1}) + \varphi_i(\varphi_{t2}), \ldots, \varphi_i(\varphi_{tn})\}$ such that φ_i is the sum of transmission power spectral impact (φ_{tp}) and interference generated by the SUs after selecting similar channel band in the region r_i.

In our scheme, the data capacity (φ_{dc}) of a channel $\varphi_{c(i)} \in \Sigma\{\varphi_{cn}\}$ is one of the primary criteria to fulfill the requirement of applications can be formally calculated as follows

$$\varphi_{dc(\varphi_{sui}, \varphi_{psj})}^{C(i)} = \varphi_{b(i)}\varphi_{log(i)}\left(1 + \frac{\varphi_p}{(\varphi_{n0}\varphi_{b(ci)})} \times \varphi_{d(\varphi_{sui}, \varphi_{psj})}\right) \bullet \Upsilon \tag{1}$$

where φ_{psj} is an active neighboring belongs to $\Sigma\{\varphi_{su}\} \cup \Sigma\{\varphi_{pu}\}$, $\varphi_{dc(\varphi_{sui}, \varphi_{psj})}^{c(i)}$ is the channel data capacity between pair of nodes (φ_{sui}, φ_{psj}), $\varphi_{b(ci)}$ is the channel i bandwidth, φ_p is the power spectral density, Υ is constant whose value is set to 0.1, and distance between pair of nodes (φ_{sui}, φ_{psj}) is indicated by $\varphi_{d(\varphi_{sui}, \varphi_{psj})}$, φ_{n0} is the noise. Here, it is noted that φ_{dc} of a channel φ_{ci} is correlated to the strength of association between a single hop pair of nodes (φ_{sui}, φ_{psj}). Stronger the associate is higher is the channel φ_{ci} reliability such that

$$\varphi_{asso.(\varphi_{sui}, \varphi_{psj})} = \sum_{\varphi_{si}}\sum_{\varphi_{sj}} \rho(\varphi_{si}, \varphi_{sj}) log \frac{\rho(\varphi_{si}, \varphi_{sj})}{\rho(\varphi_{si})\rho(\varphi_{pj})} \tag{2}$$

where φ_{si} and φ_{sj} is a particular state of the users φ_{sui} and φ_{psj} in term of distance. While one hop neighbors $\varphi_{N(n)}$ associated to a node φ_{sui} in region r_i with activate links (φ_{sui}, φ_{psj}) during time $\varphi_{t(i)}$ excluding node i itself is shown in the following formula.

$$\varphi_{N(n-i)}(r_i) = \left(\bigcup_{j \in \varphi_{N(n)}} N_j^n\right) - \{\varphi_{sui}\}, \quad j = 1, 2, \ldots, n \tag{3}$$

The effect of power spectral density, which means power is spread over the entire band is also considered as interference for other SUs. A SU find a vacant frequency band can transmit information using transmission power lie in a feasible set

$$\varphi_{ftp}^{cn} = \{\varphi_{\min\ (ftp)}^{ci}, \varphi_{\max\ (ftp)}^{ci}\} \text{for} 0 < \varphi_{miN\ (ftp)}^{ci} < \varphi_{\max(ftp)}^{ci} \tag{4}$$

where φ_{ftp}^{cn} is the set of transmission power, $\varphi_{\min\ (ftp)}^{ci}$ is the minimum transmission power used for a channel $\varphi_{c(i)}$ and $\varphi_{\max\ (ftp)}^{ci}$ is the maximum feasible power less than defined threshold value $\varphi_{th\ (ftp)}^{ci}$ is used without creating neighboring interference. The constraint of transmission energy consumption depends on the selected band. Remember that $\varphi_{\max\ (ftp)}^{ci} = \varphi_{\max\ (ftp)}^{ci}$ is the only case when a SU can transmit its data on its designated band only if all neighbors goes silent. Thus, interference constraint can be computed as:

$$\varphi_i = \frac{\varphi_{tp(sui)}^{ci}\varphi_{h(sui,psj)}^{ci}}{\sum_{i \neq j}\varphi_{tp(psj)}^{ci}\varphi_{h(sui,psj)}^{ci}} \tag{5}$$

where $\varphi_{tp(sui)}^{ci}$ and $\varphi_{tp(psj)}^{ci}$ are the SUs and PUs vectors indicate the transmission power consumption over channel φ_{ci}. $\varphi_{h(sui \bullet psj)}^{ci}$ is the gain between node pair (sui, psj) for channel $\varphi_{c(i)}$. To maximize the total utility summed over all users, we assume that function $\psi_{sui}(\varphi_{ci}^{sui}) = \phi_{sui}\log(1 + \varphi_{ci}^{sui})$ is proportional to Shannon capacity of the secondary user i's channel weighted by dependent priority parameter ϕ_{sui} of the user. Thus, utility for each user's channel selection and power allocation, i.e.,

$$\max_{\varphi_{ci},\ \varphi_{tp}^{sui}} \psi_{tot}(\varphi_{tp}) = \sum_{i=1}^{n} \psi_{sui} \bullet \mu(\varphi_{ci}^{sui}(\varphi_{tp}^{sui})) \tag{6}$$

where μ is a constant factor whole value is set to 0.01.

By understanding the channel selection interference problems, we assume that each secondary user φ_{sui} in the region r_i chooses the only one suitable channel from the available channel list. To minimize the interference impact such that $\varphi_{sui}^{ci} \cap \varphi_{psj}^{cj} = \varnothing, i.e., \varphi_{f(sui)} + \varphi_{f(psj)} \leq 1$ where $\varphi_{f(sui)} = 1/\Sigma\{\varphi_{cn}\}$ and $\varphi_{f(psj)} = 1/\Sigma\{\varphi_{cn}\}$ for $\{\varphi_f = \varphi^{ci}\}$, are the normalized spectrum assigned to different users. Consequently, the constraint for each user φ_{sui} is to limit every neighbor ($\varphi_{N(i)}$) of φ_{sui} to use different spectrum channels (φ_{sc}), which can numerically described as

$$\varphi_{sc} = \varphi_{sui}^{ci} + \sum_{j \in N(i)} \varphi_{sui}^{ci} \leq 1, i = 1, 2, \ldots, n \tag{7}$$

subject to

$$\varphi_{sc} = \varphi_{sui}^{ci} + \sum_{j \in N(i)} \varphi_{suj}^{cj} \leq 1, i = 1, 2, \ldots, n for \varphi_{th(sui)} < \varphi_{th(suj)} \tag{8}$$

where $\varphi_{th(sui)}$ and $\varphi_{th(suj)}$ is the throughput of user i and j competes for the common channel can be measured as:

$$\varphi_{th(suj)} = \sum_j max(\lambda_j, \varphi_j^{ci}) \tag{9}$$

where λ_j is the data packet arrival rate at node j and φ_j^{ci} is the probability that node j may access the common channel φ^{ci}. Then noise in the system can be measured based on the following factors

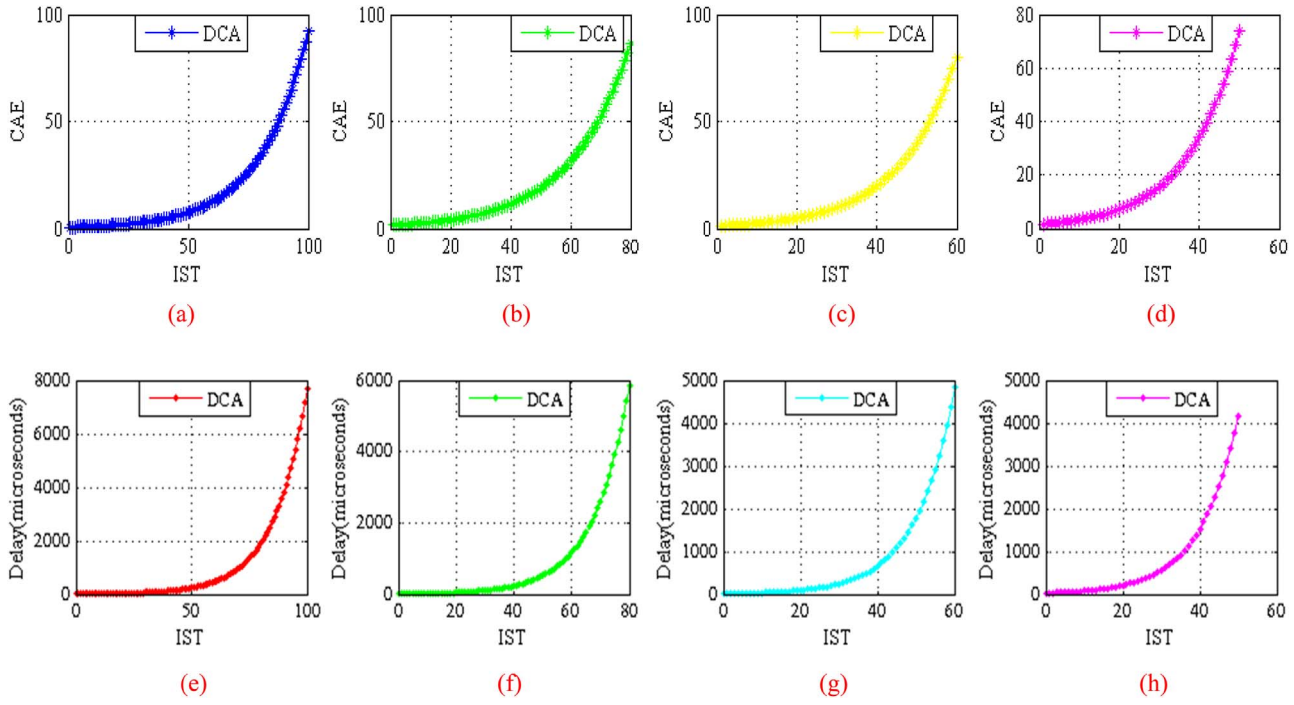

Fig. 1. shows that the channel assignment efficiency (*CAE*) is directly associated with the number of iterations stored in the channel history table (*IST*) for both automated demand supply and smart metering applications. Herein, (a) shows that the channel assignment efficiency is extremely high up to 95.150% when 100 iterations are stored in channel information table. However, this high efficiency rate is decreases rapidly up to 89.011%, when number of stored iterations are reduced up to 80 as shown in (b). Similarly, it is realized that the channel assignment efficiency rate becomes low up to 83.103% and then to 78.151%, when number of iterations are stored 60 and 50 in the information table as shown in (c) and (d), respectively. Also, the channel assignment delay is directly linked with the number of iterations stored in the channel history table (*IST*). Herein, (e) shows that the channel assignment delay is between 7600 and 7900 μs when 100 iterations are stored in channel information table. However, this delay rate is rapidly decreases between 5800 and 6000 μs when numbers of stored iterations are reduced up to 80 as shown in (f). Similarly, it is observed that the channel assignment delay become extremely poor between 4800 and 5000, and 4000 and 4300 μs when number of iterations are stored 60 and 50 in information table as shown in (g) and (h), respectively.

$$\varphi_{n0}(\varphi_m) = \varphi_{en0}(\varphi_{ti}) + \varphi_{hmn0}(\varphi_{ti}) + \varphi_{emn0}(\varphi_{ti}) + \varphi_{mn0}(\varphi_{ti}) \tag{10}$$

where $\varphi_{en0}(\varphi_{ti})$ shows environmental conditions (i.e., temperature, moisturizer, etc., based on the deployment field), $\varphi_{hmn0}(\varphi_{ti})$ shows human or mammal noise, $\varphi_{emn0}(\varphi_{ti})$ denotes the effect of electromagnetic signals in the field and $\varphi_{mn0}(\varphi_{ti})$ illustrates the machine or system noise. Aforesaid that in the designed scheme based on prior channels history desired channels are assigned to SUs with higher stability, that is, longer idle probability. Therefore, each node i maintains the channel history (h) of PUs from the sensing results based on the user defined priority (pi) can be numerically written as:

$$\varphi^{i}_{pu(h)} = \sum\nolimits_{\varphi_{cn}} [\varphi^{pi}_{ci}], \quad i=1, 2, ..,n \tag{11}$$

where $\varphi^{i}_{pu(h)}$ is the PU activity vector and φ^{pi}_{ci} are the channels stored with priority in decreasing order during time φ_{ti}.

$$\varphi^{i}_{pu(h)} = \sum\nolimits_{\varphi_{ci}} [\varphi^{pj}_{ci}], \quad j=1, 2, ..,n \tag{12}$$

where φ^{pj}_{ci} is history vector of a specific channel φ_{ci} observed in specific time intervals $\varphi_t = \{\varphi_{t1}, \varphi_{t2}, \ldots, \varphi_{tn}\}$. The value of φ_t in vector form can be indicated as:

$$\varphi^{i}_{pu(h)} = \begin{bmatrix} \varphi_1^1 \varphi_2^1 \varphi_3^1 & \varphi_t^1 \\ \varphi_1^2 \varphi_2^2 \varphi_3^2 \cdots & \varphi_t^2 \\ \varphi_1^3 \varphi_2^3 \varphi_3^3 \cdots & \varphi_t^3 \\ \vdots \ \vdots \ \vdots \cdots & \vdots \\ \varphi_1^j \varphi_2^j \varphi_3^j & \varphi_3^j \end{bmatrix} \tag{13}$$

Thus, based on prior history the transition probability matrix of channel φ_{ci} can be numerically expressed as:

$$\varphi_{ci(h)} = \begin{bmatrix} \varphi_{ci\ (0,0)} \varphi_{ci\ (0,1)} \leftarrow & \varphi_F \\ \varphi_{ci\ (1,0)} \varphi_{ci\ (1,1)} \leftarrow & \varphi_B \end{bmatrix} \tag{14}$$

where φ_F and φ_B represent channel is free or busy respectively, and 0 indicate idle state while 1 shows busy state. The transition probability matrix of all channel φ_{cn} can be indicated as:

$$\varphi_{cn(h)} = \begin{bmatrix} \varphi_{ci\ (0,0)} \varphi_{cj\ (0,0)} \varphi_{ck\ (0,0)} \cdots & \varphi_{t1} \\ \varphi_{ci\ (0,1)} \varphi_{cj\ (0,1)} \varphi_{ck\ (0,1)} \cdots & \varphi_{t2} \\ \varphi_{ci\ (1,0)} \varphi_{cj\ (1,0)} \varphi_{ck\ (1,0)} \cdots & \varphi_{t3} \\ \vdots \quad \vdots \quad \vdots \quad \vdots & \vdots \\ \varphi_{ci\ (1,1)} \varphi_{cj\ (1,1)} \varphi_{ck\ (1,1)} \cdots & \varphi_{tn} \end{bmatrix} \tag{15}$$

For given facts, we can also calculate the probability of distinct channel values access stored in channel table by assuming that entire history $\{\varphi_{h1}, \varphi_{h2}, \ldots, \varphi_{hn}\}$ of a channel φ_{cj} such that $\varphi_{ci} \in \sum_{\varphi_{h(ci)}} \{\varphi_{h1}, \varphi_{h2}, \ldots, \varphi_{hn}\}$ from the entire prior history set $\varphi_{h(cn)} \in \sum_{\varphi_{h(cn)}} \{\varphi_{ch1}, \varphi_{ch2}, \ldots, \varphi_{chn}\}$, i.e.,

$$\rho(\varphi_{cj}, l) = \frac{(\Sigma \varphi_{h(ci)} \cdot \varphi_{tri})^{\varphi_{cj}}}{\Sigma(\varphi_{h(cn)})} \, exp(-\varphi_{tri} l) \, for \text{ simplicity } l = \varphi_{cj}/\varphi_{cn} \tag{16}$$

The increase in size of the channel history table may also increase the channel selection reliability, is a tradeoff with memory requirement and table management complexity. Therefore, we consider first in old out (FIOL) policy, which means that a channel history not used for after defined time threshold $\varphi_{t(th)}$ will be swapped in the light of new information for a cycle can be identified as:

$$\int_{t_1}^{t_2} \varphi_{N(t)} dt = \sum_{i=1}^{n} \varphi^{ci}_{ts(psi)} \geq \varphi^{ci}_{t(th)} for \varphi^{ci}_{(psi)} \tag{17}$$

subject to

$$\int_{t_0}^{t_n} \varphi_{N(t)} dt = \sum_{i=1}^{n} \varphi^{ci}_{ts(psi)} \tag{18}$$

where $\varphi_{N(t)}$ is the total number of channel information stored between time t_0 and t_n, φ_{ts}^{ci} is the residing time of a channel i for the primary user or secondary user (psi), t_1 and t_2 is the time when channel information of a user $\varphi_{ts(psi)}^{ci}$ is swapped with $\varphi_{(psi)}^{ci}$ in the light of new information by following time threshold $\varphi_{t(th)}^{ci}$ value. This process avoids the channel table management complexity. In our scheme, to overcome the desired data capacity channel scarcity issues, if a node does not have desired capacity channel information or current is occupied then it may also negotiate to its single hop neighboring nodes in region r_i instead of sensing the entire region r_n.

In each iteration, throughout the negotiation process neighboring node and channel information table is updated periodically in the light of new information. As stated earlier, this excessive message sharing may also increase the channel selection reliability with the increases in table management complexity due to large channel history table size as shown in the Fig. 1. However, this restricted channel sensing mechanism helps multiple secondary users to sense desired data capacity channel in different regions simultaneously without generated excessive interference in the smart grid. Consequently, based on prior channel history information we may also calculate the channel availability between time t_i and t_j idle for t_k times based on number of number of data packets sent (DPS) previously as:

$$\rho(\varphi_{cj} : \varphi_{tot} \geq t_k) = \frac{\rho(\varphi_{cj} : \varphi_{tot} \geq t_k)^{DPS}}{\rho(\varphi_{cj} : \varphi_{tot} \geq t_k)} \tag{19}$$

Accordingly, based on prior channel probability we may define the collision probabilities between PUs and SUs in a region (r^i) between time t_0 and t_n, such that

$$\rho_{sui}^{ci} = \int_{t_0}^{t_n} \frac{\varphi_{nc}[t_0, t_s]}{\varphi_{pui(b)}[t_0, t_s]} \tag{20}$$

and

$$\rho_{pui}^{ci} = \int_{t_0}^{t_n} \frac{\varphi_{nc}[t_0, t_s]}{\varphi_{sui(npt)}[t_0, t_s]} \tag{21}$$

In above equation, φ_{nc} is the number of collisions, $\varphi_{pui(b)}$ is busy period for PU_i and $\varphi_{sui(npt)}$ is the number of data packets transmitted for SU_i between time slot t_0 and t_s. Consequently, we may also find out the future probability of observing the collision in term of success (φ_s) and failure (φ_f) for (φ_s) + (φ_f) trails using the law of total probabilities, i.e.,

$$\rho(\varphi_s, \varphi_f) = \sum_{i=1}^{k} \rho(\varphi_s, \quad \varphi_f and \varphi_{ph} = \varphi_{psi}) \tag{22}$$

$$= \sum_{j=1}^{k} \rho(\varphi_s, \varphi_f and \rho = \rho_i)\rho(\varphi_{psi}) \tag{23}$$

$$= \sum_{j=1}^{k} \frac{\langle \varphi_s, +\varphi_f \rangle!}{\varphi_s! \varphi_f!} \varphi_{psi}^{\varphi_s} (1-\varphi_{psi})^{\varphi_f} \rho(\varphi_{psi}) \tag{24}$$

where $\rho(\varphi_{psi})$ can indicate the prior probabilities before any channel information or posterior probabilities after observing channel information history. Consequently, the longer idle probability reduces the collisions occurs between PUs and SUs and saves a significant amount of retransmission power, which is consumed during re-sensing the spectrum holes. When sensing event (φ_l, φ_i) is introduced then region $\varphi_{r(i)}$ generates a series of patterns of activity of SUs over time indicated as:

$$r^{\varphi_{r(i)}T}(\varphi_{t1}, \varphi_{tn}) \equiv \{r^{\varphi_{r(i)}T}(\varphi_{t1}), r^{\varphi_{r(i)}T}(\varphi_{t2}), \ldots, \quad r^{\varphi_{r(i)}T}(\varphi_{tn})\} \tag{25}$$

Herein, because of different data capacity channels the gain of each channel is entirely different, therefore (φ_l, φ_i) in region $\varphi_{r(i)}$ is not the same in any other region $\varphi_{r(n-i)}$, but follows a probability distribution $(r^{\varphi_{r(i)}T}(\varphi_{t1}, \varphi_{tn})|\varphi_l, \varphi_i)$. If we expect that the activity is not correlated in different regions on timescales then probability distribution can be written as a product over time as:

$$\rho(r^{\varphi_{r(i)}T}(\varphi_{t1}, \varphi_{tn})|\varphi_l, \varphi_i) = \prod_{i=1}^{n} p(r^{\varphi_{r(i)}T}(\varphi_{tn})|\varphi_l, \varphi_i(\varphi_{tn})) \tag{26}$$

For given history of activity patterns $r^{\varphi_{r(i)}T}(\varphi_{t1}, \varphi_{tn})$ by known φ_i, the optimal region $\varphi_{r(i)}$ probability distribution over φ_l given $r^{\varphi_{r(i)}T}(\varphi_{t1}, \varphi_{tn})$, then using Bayes' rule posterior distribution is computed as:

$$\rho(\varphi_l|r^{\varphi_{r(i)}T}(\varphi_{t1}, \varphi_{tn}), \varphi_i) \propto \prod_{i=1}^{n} \frac{p(r^{\varphi_{r(i)}T}(\varphi_{tn})|\varphi_l, \varphi_i)}{p(r^{\varphi_{r(i)}T}(\varphi_{tn})|\varphi_i)} \tag{27}$$

Since the beginning of the trial this distribution captures and retains all the information in the $r^{\varphi_{r(i)}T}$ activity. If we encode a posterior distribution $p(\varphi_l|r^{\varphi_{r(i)}T}(\varphi_{t1}, \varphi_{tn}))$ and ignore the effect of φ_l then connections between SUs activities φ_a and region $r^{\varphi_{r(i)}T}$, probability distributions such that

$$\rho(\varphi_l|r^{\varphi_a}(\varphi_{tn})) = p(\varphi_l|r^{\varphi_{r(i)}T}(\varphi_{t1} : \varphi_{tn})) \tag{28}$$

The optimal network connectivity depends on how the information about the SUs activities is denoted in a region $r_i^{\varphi_{su(n)}T}$, which in turn associated with the variability of channel selection. Thus, the probability of entire history of $r_i^{\varphi_{su(n)}T}$ activity can be numerically expressed as:

$$\rho(\varphi_l|r^{\varphi_{r(i)}T}(\varphi_{t1}, \varphi_{tn})) \propto exp\left(h(\varphi_l) \bullet \sum_{i=1}^{n} r^{\varphi_{r(i)}T}(\varphi_{tn})\right) \tag{29}$$

Consequently, the probability of entire network activity is modeled can be numerically expressed as:

$$\sum_{i}^{n} r^i \left(\rho(\varphi_l|r^{\varphi_{r(i,)}T}(\varphi_{t1}, \varphi_{tn})) \propto exp\left(h(\varphi_l) \bullet \sum_{i=1}^{n} r^{\varphi_{r(i)}T}(\varphi_{tn})\right)\right) \tag{30}$$

where $h(\varphi_l)$ is the history of the sensing event and $r^i \in \forall\ i = 1,2,\ldots,n$.

2.3. Fish bone routing algorithm (FBR)

In smart grid deployment environment, one of the key challenges for research is to design a routing protocol that provides application-specific service guarantees. In several WSN-based smart grid applications monitored data must be delivered within a certain period of time from the moment it is sensed, otherwise the data will be useless. Therefore, the basic application-specific requirement in smart grid sensor network is to guarantee efficient delivery of critical information in a timely manner even when the network facing a certain percentage of loss. This single or a set of nodes failure must not affect the overall monitoring tasks to reflect the recent physical view of the sensing environment in smart grid. Thus, the designed routing scheme must be capable of to establish new reliable links on immediate basis without interruption and routes data packets towards sink with high priority. In addition, the designed scheme must also preserve sensor nodes available resources efficiently to distribute energy consumption load evenly for long-term applications deployment in smart grid. This might needs re-routing data packets through the different regions where more energy is available or actively adjusting transmit powers and signaling rates on the existing links to minimize energy consumption in the smart grid sensor network. Considering the above important challenging issues, in the second phase of our proposed scheme a fish bone routing algorithm plays an important role by providing a quality aware stable routing architecture to reflect the recent physical view of the sensing environment in smart grid. In proposed routing algorithm, multiple fish bone routing architectures are constructed to provide efficient data delivery even when the network is facing a certain percentage of loss. To increase computational efficiency, we employed shortest path backbone routing architecture to identify all available paths for from the source to destination in the network. Its simple and

Table 2
Notations used in FBR.

Notation	Description
$\varphi_{Rsd}(G, \rho)$	is reliability on network G with probability ρ between source (s) and destination (d)
$\rho(\Phi_i)$	is the probability calculated for a set of isolated data paths for $\{i = 1,2,\ldots,n\}$
$\rho(\mathcal{E}_i)$	is the probability of a available data path $\mathcal{E}_i$ from source towards destination
$\rho(\overline{\mathcal{E}}_i)$	is the complementary probability of a available path $\mathcal{E}_i$ from the source to destination
$\rho(\varphi_{lsn(ij)})$	is the reliability probability for a set of links l_{ij} between each pair of sensor node i and j
$\overline{\varphi}_{fsn(ij)}$	is the estimated link data flow between sensor node i and j in the fish backbone network.
$\breve{\varphi}_{fsn(ij)}$	is the observed link data flow between sensor node i and j in the fish backbone network.
$\overline{\varphi}_{fsd(ij)}$	is the estimated data flow from the source to destination having n sensor nodes in the fish backbone network.
$\breve{\varphi}_{fsd(ij)}$	is the observed data flow from the source to destination having n sensor nodes in the fish backbone network.
$\varphi_{sn(ik)}$	is the shortest path between source sensor node i to sensor node k towards sink
$\varphi_{crsd(ij)}$	is the connective reliability between sensor node i and sensor node j over a particular source and destination pair.

distributed workload nature helps to prevent energy depletion by exploiting nodes density in the network. Herein, observed information always routed in greedy manner over the highly stable links formed among the backbone and ribs nodes in the network. During data forwarding phase, after receiving information each backbone node looks into its routing table and selects next hop node with the minimum transmission distance, energy level and node angle information. In term of a route node failure, prior history stored in the routing table helps to find an alternative quality aware data path rapidly with least delay in the network. The entire route construction process in fishbone architecture is divided into various sections given below: (Table 2).

2.3.1. Fish backbone construction

A sink node is responsible to initiate multiple fish backbone route construction process by sending route construction message request (msg_r_c) to its neighboring nodes in the network. After receiving the first route construction request message by the destination node, sink starts a timer for the route selection time window. Each node after receiving route construction message request computes its weighting factor value ($\varphi_{\text{sni}}^{wf}$) and sends this information via reply message ($reply\_r_c$) in time ($\varphi_{t(i+j)}$) using CSMA mechanism. Generally, this weighting factor is based on the node residual energy (φ_{Esni}), distance to neighbors ($\varphi_{d(snij)}$) and angle information ($\varphi_{A(snij)}$). Then after a specific time interval ($\varphi_{t(i+k)}$) sink node sends acceptance message ($neigh.\ \_r_c$) to single hop neighboring nodes have maximum weight factor value. This figured information of each sensor node is stored in decreasing order in the constructed routing table of the sink. This entire process repeats and at each hop and a next hop node is selected with the highest weight value until the entire multiple fish backbone like routing architecture with least cost is constructed within the defined timer window expires.

2.3.2. Fish ribs construction

After multiple fish backbone routing architectures formation each backbone node ($\varphi_{\text{sni}}^{B_i}$) is responsible to appoint multiple rib nodes to complete fishbone network. To complete this process, each backbone node ($\varphi_{\text{sni}}^{B_i}$) sends its rib message request (rib_r_c) to its neighboring nodes in range in time interval ($\varphi_{t(l+1)}$). After receiving rib message request each node in range computes its weighting factor value and sends this information to backbone node via rib reply message ($ribreply\_r_c$) in time interval ($\varphi_{t(l+j)}$). Then after a specific time interval ($\varphi_{t(i+k)}$) each backbone node replies to its one hop neighboring nodes have highest weighting factor value via rib acceptance message ($rib.\ \_r_c$). This computed information of each sensor node is stored in decreasing order in the constructed routing table of the backbone nodes. This entire process repeats and at each hop a next hop node is selected with the highest weight value until complete fish bone like routing architecture is constructed in the network. Herein, we restricted multi-hop rib node network maximum up to three hopes. Moreover, it is important to note that the angle information of the rib and backbone nodes can be entirely different from each others based on the user defined deployment policies.

Let consider a network of n sensor nodes, i.e., $\sum_{\varphi_{sn}}\{\varphi_{sn1}, \varphi_{sn2}, \ldots, \varphi_{sn}\}$ having coordinate information (x_i, y_i) and (x_j, y_j) to the origin (x_k, y_k) in the positive region. The nodes in the backbone architecture are denoted as $\sum_{\varphi_{sn1}^{B_n}}\{\varphi_{sn1}^{B_i} | i1,2,\ldots,n\}$ while sensor nodes in the ribs architecture are indicated as $\sum_{\varphi_{\text{sn}1}^{R_n}}\{\varphi_{\text{sn}1}^{R_i} | i1,2,\ldots,n\}$. The pair of link $l(ij)$ between a set of sensor nodes $(\varphi_{sn(ij)})$ in the network are indicated as $\sum_{\varphi_{lsn(ij)}}\{\varphi_{lsn(i)} | i1,2,\ldots,n\}$. We assigned each node in the network a specific weight (φ_{wi})as $\sum_{\varphi_{sn1}^{wn}}\{\varphi_{sn1}^{w1}, \varphi_{sn2}^{w2}, \ldots, \varphi_{sn}^{wn}\}$ based on the energy level information, i.e., $\sum_{\varphi_{Esn}}\{\varphi_{Esn1}, \varphi_{Esn2}, \ldots, \varphi_{Esn}\}$,Euclidean distance to neighboring nodes as $\sum_{\varphi_{d(snij)}}\{\varphi_{dsn(j)} | j1,2,\ldots,n\}$ and angle information (φ_A) denoted as $\sum_{\varphi_{A(sni)}}\{\varphi_{Asn(j)} | j1,2,\ldots,n\}$. Then the weighting factor for a sensor node i in fish backbone routing network (B) numerically can be indicated as:

$$B\varphi_{\text{sni}}^{wj} = \left(\frac{1}{\varphi_{dsn(ij)} + \varphi_{A(snij)}}\right) \times \varphi_{\text{Esnj}} \tag{31}$$

where the weighting factor for the rib (R), single hop nodes can be formally written as:

$$R\varphi_{\text{sni}}^{wj} = \left(\frac{\varphi_{A(snij)}}{\varphi_{dsn(ij)}}\right) \times \varphi_{\text{Esni}} \tag{32}$$

while the weighting factor of the single hop node to the next hop (N_h) can be numerically expressed as:

$$N_h\varphi_{\text{sni}}^{wk} = \left(\frac{1}{\varphi_{dsn(jk)} + \varphi_{A(snjk)}}\right) \times \varphi_{\text{Esnk}} \tag{33}$$

The structural degree of a sensor node i for the ribs and single to next hop nodes can be computed as:

$$\varphi_{A(sni)} = \sum_{j=1}^{m} \varphi_{\text{sn(ij)}}^{wi} \tag{34}$$

subject to

$$\varphi_{A(snij)} = tan^{-1}\left|\frac{y_j - y_i}{x_j - x_i}\right| for x_j > x_i \tag{35}$$

$$\varphi_{dsn(ij)} = \sqrt{|x_j - x_i|^2 + |y_j - y_i|^2} \tag{36}$$

$$\varphi_{\text{Esnj}} = |\text{I}_{\text{Esnj}} - \text{C}_{\text{Esnj}}| \tag{37}$$

where m is the neighbors set of nodes i, φ_{Esnj} is the residual energy of a node j, I_{Esnj} is the initial node energy, C_{Esnj} is the node j utilized energy and d_{th} is the threshold distance.

2.3.3. Route discovery

In route discovery process, a source node needs to start a communication sends its route request message (REQ) to neighboring node having highest weight value in the routing table. When an intermediate node receives this route request packets if available then it replies to sender node via request packet (RREQ) along with available time slot information for reliable communication. In a case, if a next hop does not reply in defined time interval t_i then a next hop node with second highest weighting value is selected to convey information in greedy manner from source towards destination. This entire process repeats until the observed information is reached from the source to sink.

2.3.4. Fishbone network reliability

The reliability of a routing network could be defined distinctly based on the application-specific service requirements in smart grid. In our scheme, the term reliability is the probability of successful delivery of the critical information from the source (s) to destination (d) within a given time period (φ_n). Herein, a set of reliability measures such as source to destination reliability (φ_{Rsd}) which includes sensor node reliability (φ_{Rn}), node data flow reliability (φ_{Rnf}), routing path system reliability (φ_{Rsys}) and reliability of data flow (φ_{Rsf}) of a certain data path in the fishbone routing network. These reliability measures help to inspect the network vulnerability from the source node towards a destination in fish routing network. First, from the source to destination reliability (φ_{Rsd}) numerically defined as:

$$\varphi_{Rsd}(G,\rho) = \sum_{i=1}^{n} \rho(\Phi_i) \tag{38}$$

$$\rho(\Phi_i) = \prod_{i=1}^{n} \rho(\overline{\mathcal{E}}_{i-1}) \bullet \rho(\mathcal{E}_i) \text{ where } \mathcal{E}_i = \prod_{i=1}^{n} \rho(\varphi_{lsn(ij)}) \tag{39}$$

The computed reliability (φ_{Rsd}), is the sum of the probabilities of $i$isolated backbone path $\rho(\Phi_i)$ from the source to destination. Herein, the isolated backbone paths are mutual but statistically autonomous are estimated based on the available data paths $\mathcal{E}_i$ between source and destination in fishbone routing network. Based on the multiplication of $\rho(\varphi_{lsn(i)})$, the reliability of each isolated shortest backbone paths $\mathcal{E}_i^1$, $\mathcal{E}_i^2$, $\mathcal{E}_i^3$, $\mathcal{E}_i^4$ and $\mathcal{E}_i^5$ as $\rho(\mathcal{E}_1)$,$\rho(\mathcal{E}_2)$,$\rho(\mathcal{E}_3)$,$\rho(\mathcal{E}_4)$ and $\rho(\mathcal{E}_5)$ is computed to remove the shared probability among $\mathcal{E}_i$ within each state vector. This entire mechanism effectively helps to remove doubly computed probabilities of the shared links among $\mathcal{E}_i$ and makes all routes mutually and statistically separated in the fishbone routing network. It also helps to find the probability initial $\rho(\mathcal{E}_i)$ of other unused paths $\mathcal{E}_i$ for any initial $\rho(\mathcal{E}_i)$. To evaluate the node reliability among the Nsensor nodes, we first computed the range between the lowest ($\varphi_{min.R}$) and highest reliability ($\varphi_{max.R}$) at each sensor node i and its average reliability from different sources to a specific destination (sink), respectively. Then, we define the system reliability with average reliability from all sources s_i to a certain destination d of the fish backbone network such that

$$\varphi_{Rn}(G,\rho) = \frac{1}{(N-1)} \sum_{i=1}^{n} \varphi_{R_{Si}d} \text{ whered } \in sink \tag{40}$$

$$\varphi_r(G,\rho) = |max\varphi_{R_{Si}d} - min\varphi_{R_{Si}d}| \tag{41}$$

The average shortest path (φ_{ASP}) for Nnumber of sensor nodes is the length of a shortest path from a node i to sensor node k in a given fish backbone routing network. It reflects the internal structure of a fish backbone routing network because it contains the internal separations of all sensor node pairs, therefore is essential to the topology and communication efficiency of a network, i.e.,

$$\varphi_{ASP} = \frac{1}{N(N-1)} \sum_{i \neq j} \varphi_{sn(ik)} \tag{42}$$

In shortest path fish backbone routing, connectivity reliability (φ_{cr}) is one of the main challenging issues for efficient and effective data delivery in the network. It is the sum of the probability of a network in which at least an effective data path between source and destination exists and is given as follow

$$\varphi_{cr} = \frac{1}{N(N-1)} \sum_{i,j \in N}^{i \neq j} \varphi_{crsd(ij)} \tag{43}$$

As observed, in fish backbone routing architecture it is also possible that a certain amount of nodes having very close distance to their neighboring nodes are in sleeping mode during forwarding data packets. Hence, the number of active and sleeping sensor nodes can be regarded as the number of pieces of witnessed link flow information to avoid unnecessary multihop data transmission in the network. Thus the decision variable can be represented in terms of 1 and 0 as:

$$\varphi_{lfi} = \sum_{ij \in l} (\varphi_{Alsn(ij)} + \varphi_{Ilsn(ij)}), \quad \forall i, j \quad \in N \tag{44}$$

where $\varphi_{Alsn(ij)}$ and $\varphi_{Ilsn(ij)}$ represents the active and inactive links between sensor node i and j, such that

$$\varphi_{Asn(ij)} = \begin{cases} 1, & if link ij is equipped with \varphi_{Alsn(ij)} \\ 0, & otherwise; \end{cases} \tag{45}$$

$$\varphi_{Isn(ij)} = \begin{cases} 1, & if link ij is equipped with \varphi_{Ilsn(ij)} \\ 0, & otherwise; \end{cases} \tag{46}$$

Considering the above information, we may also find the path coverage information (φ_{pci}) given as:

$$\varphi_{pci} = \sum_{ij \in l} \varphi_{Asn(ij)} \bullet d(p^i, \varphi_{pij}), \quad \forall \quad p^i \in \varphi_p \tag{47}$$

where the p^i is a particular data path from source towards destination containing sensor node i and j as (φ_{pij}).

While the path trajectory information (φ_{pti}) at various links along this specific path from the source to destination can be computed as:

$$\varphi_{pti} = \sum_{p \in P} \sum_{p \in P} \varphi_{Asn(ij)} \bullet \quad \varphi_{pij} \tag{48}$$

For the known rate of data packets flow (φ_{Dsd}) between the source and destination the node data flow ($\varphi_{f(sni)}$) from a specific source to all other destinations can also be derived as:

$$\varphi_{nf}(G,\rho) = \sum_{d=1}^{n} \varphi_{Dsd} \bullet \varphi_{f(sni)} \tag{49}$$

where the gap between uppermost and lowermost traffic flows at a given node for a certain data path can be numerically indicated as:

$$\varphi_{fr}(G,\rho) = |max\varphi_{Dsd}\varphi_{Rsd} - min\varphi_{Dsd}\varphi_{Rsd}| \tag{50}$$

The link flow estimation error between sensor node i and j associated to a particular source and destination pair in the fishbone routing network can be numerically calculated as:

$$\varepsilon(\overline{\varphi}_{fsn(ij)}) = mape(\overline{\varphi}_{fsn(ij)}) = \frac{|\breve{\varphi}_{fsn(ij)} - \overline{\varphi}_{fsn(ij)}|}{\breve{\varphi}_{fsn(ij)}} \bullet 100\% \tag{51}$$

$$\varepsilon(\overline{\varphi}_{fsd(ij)}) = mape(\overline{\varphi}_{fsd(ij)}) = \frac{|\breve{\varphi}_{fsd(ij)} - \overline{\varphi}_{fsd(ij)}|}{\breve{\varphi}_{fsd(ij)}} \bullet 100\% \tag{52}$$

By taking into account the complementary probability of (φ_{Rsd}) the entire network system flow loss among all source and destination pairs ($\varphi_{l(sd)}$) to examine the network resilience can be computed as:

$$\varphi_{l(sd)}(G,\rho) = \sum_{s=1}^{n} \sum_{d=1}^{n} \varphi_{Dsd}(1 - \varphi_{Rsd}) \tag{53}$$

In sum, computed probability shows the true reliability (φ_{Rsd}) of the

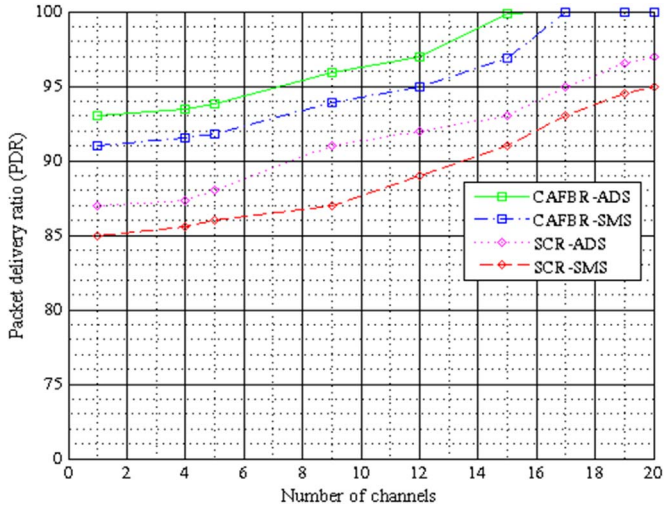

Fig. 2. Packet delivery ratio vs number of channels between 1 and 20.

available data paths, which means that the generated data packets flow from the source towards destination don't encounter any excessive delay above the defined threshold due to construction of highly reliable link quality aware data paths in the fishbone routing network.

3. Path loss model

In this study, we used log-normal shadowing path-loss model presented in [2]. The main reason to adopt this model is due to its providing more accurate multipath channel estimation results compared to the Nakagami and Rayleigh models in a smart grid environment. The mathematical form of the log normal shadowing model can be numerically expressed as:

$$\gamma(d)_{dB} = P_t - PL(d_0) - 10\eta log_{10}\frac{d}{d_0} - X_{\sigma - P_\eta} \tag{54}$$

where $\gamma(d)$ represents signal to noise ratio,Pt is the transmit power in dBm, $PL(d_0)$ shows the path loss at a reference distance d_o, ηindicates the path-loss exponent, X_σ denotes a zero mean Gaussian random variable with standard deviation σ, and P_η express the noise power measured in dBm. Herein, we set values of path loss exponent (n) for both line of sight and non-line of sight as 2. 43 and 3.53, respectively. While the Shadowing deviation and Noise floor for both line of sight and non-line of sight was set to 3. 12, 2.95, -89.5 and -93.5, respectively.

4. Simulation model and performance evaluation

The required information can be provided to utilities by sensor systems to enable dynamic power management and for the successful operations of the smart grids. In smart grid, diverse WSN-based SG applications have diverse QoS requirements as shown in Table. 1 (see Section-1). For instance, the latency-tolerant information exchange between the meters and utility management center is the basic requirement for smart metering applications. On the other hand, communications among substations and intelligent electronic devices require low-latency and high-data-rate in order to timely detect and isolate faults. The impact on these evaluation parameters for real-time critical, e.g., automated demand supply (ADS) and smart metering systems (SMS) applications is investigated in the evaluation Section 5. The diverse QoS requirements for both WSN-based automated demand supply and smart metering systems applications in terms of data rate and reliability also have been summarized in Table. 1.

In this study, performance evaluations were realized using a network simulation tool named EstiNet9. 0 [26] to evaluate the performance of LRP against the QoS routing protocol named SCR [27] proposed for WSN-based smart grid applications using four widely used metrics: (i) packet delivery ratio (PDR), (ii) delay, (iii) throughput, and (iv) residual consumption. PDR is regarded as the ratio between the number of packets successfully received by the sink and those sent by the source nodes. Delay is the time taken by a packet to reach any destination node from a source node. Throughput is the number of data packets processed in a given time (bits per second). Residual energy is the amount of remaining energy after energy consumed during successful transmission of data packets by the nodes. Consequently, in our simulation study we consider total number of sensor nodes 250 equipped with physical layer standard IEEE802.11b having maximum data rate of 283 kbits/s. These sensor nodes are deployed in 2D (length × width) area with values (800 × 600) meters with the sink chosen at the corner of the grid. In smart grid, each node is considered as responsible to obtain a certain view of the employment. However, it can only cover a limited physical area of the environment due to its limited both in range and in accuracy characteristics. Therefore, to satisfy entire network coverage problem the maximum communication range of each sensor node in cognitive radio network is set to maximum 100 m in the network. The initial energy, data aggregation, idle listening, sleeping and receiving power is set to 4.5 J, 0.043 W, 0.083 W, 3×10^{-6} W and 0.35 W, respectively. Herein, we divided the communication energy consumption into two categories 0.083 W for small and 0.97 W for long range communication. In addition, we set data packet length to 38 bytes. The performance evaluations consist of 51 sets of simulations.The fraction of the each routing protocol originated data packets deliver to sink for both automated demand supply (ADS) and smart metering systems (SMS) is shown in Fig. 2. During experimental studies, we observed that the PDR of CAFBR in both ADS and SMS is dependent of offered traffic load and deliver data up to 93% and 91% of the originated data packets when default channel is assumed in the deployed network, respectively. However, this PDR rapidly increases and reaches up to 100% when the number of channels are assumed 15 and 17 for both ADS and SMS applications, respectively. Similarly, the PDR of SCR for both ADS and SMS is observed up to 83% and 80% of the originated data packets when default channel is assumed in the deployed network, respectively. This packet delivery also increases in SCR and reaches up to 93% and 90% when number of channels are assumed 20 for both ADS and SMS applications. Herein, it is observed that the SCR in both scenarios fail to achieve high PDR because its routing table entries directed sensor nodes to forward data packets over unreliable links, which drops a significant amount of data packets in the network. Moreover, it does not consider appropriate channel utilization for reliable data delivery in smart grid. Generally, in SCR each node is responsible to maintain only one or two routes per effective next hop for conveying data packets, hence at each hop data packet that the MAC (Medium Access Control) layer is unable to deliver is dropped since there are no more alternative routes lead to the destination. In SCR, the successful transmission becomes more improbable as the intermediate hop counts are increased in the routing path of the deployed network in both ADS and SMS applications. Here, we expect if the route length increases, then number of intermediate unnecessary hops also increased which makes a certain amount of data packets invalid due to not delivering at a defined threshold time to sink. For a given time an internal mechanism of our network simulator knows the length of the shortest possible path between all source and destination in the smart grid network. It is responsible to label all data packets with their path length and also the origin, destination and time when they are originated in the network. To measure the actual delay effect caused by the difference between the paths actually taken by data packets and this shortest path length in both routing schemes. Here, we consider high delay effect if a difference is greater than 0, which means that the numbers of extra hops are included in the routing path while the difference of 0 means the packet took optimal or near the best shortest path. Realizing the

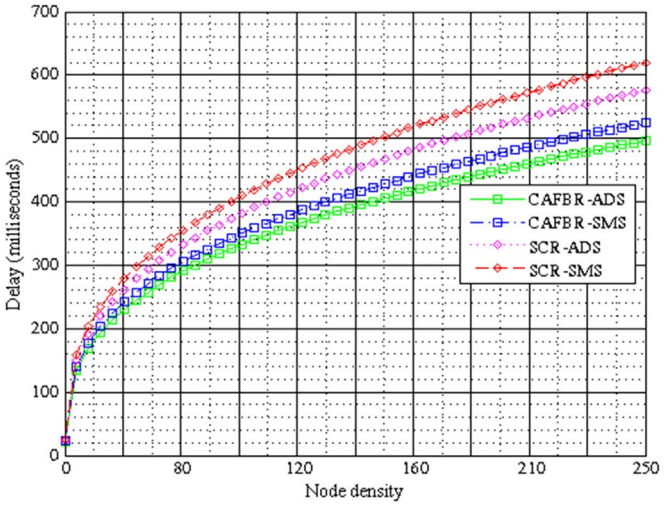

Fig. 3. Delay vs nodes density between 1 and 250.

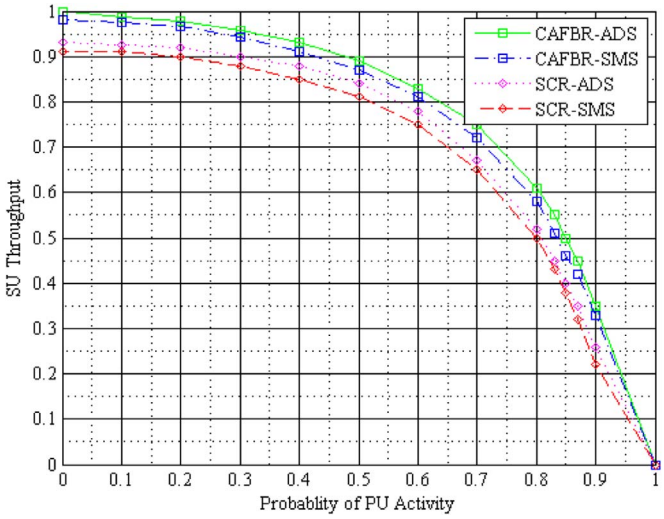

Fig. 4. Secondary user throughput vs primary user activity.

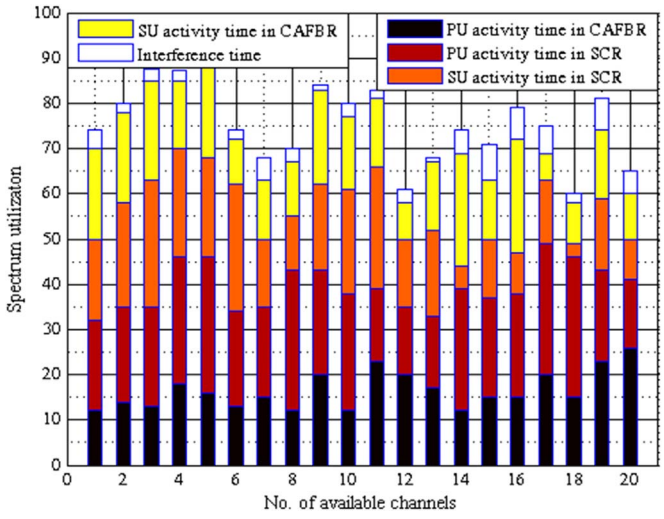

Fig. 5. Spectrum usage vs number of channels between 1 and 20.

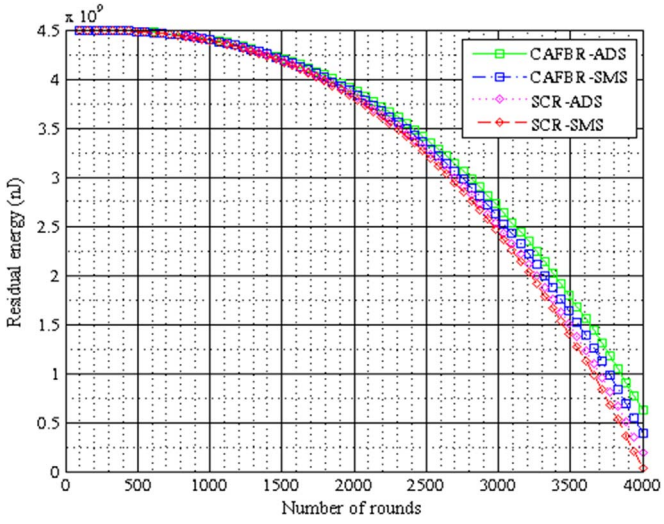

Fig. 6. Residual energy vs number of rounds between 1 and 4000.

obtained experimental data, we found that CAFBR uses routes very close to the defined number of hops as designed to find shortest paths in both ADS and SMS scenarios. On the other hand, SCR has a significant tail for some packets, taking up to 6 or more hops longer than optimal number of hops. Thus, in SCR a certain amount of data packets are dropped due to the creation of path loops from source to destination in the network which is found more for SMS than ADS applications. The data packets in loops may also possibly cause interfere with the other nearby nodes to successfully exchange the broadcast and cause more packets to be dropped in the network thus PDR is reduced poorly. Thus, one of the major challenging issues which leads to increasing network delay is unnecessary multi-hop data transmission which directly or indirectly affects high PDR in SCR in both ADS and SMS scenarios. Moreover, in SCR a certain amount of data packets are dropped due to the creation of path loops from source to destination in the network which is found more for SMS than ADS applications. Fig. 3 make it clear that our proposed scheme compared to SCR has to face low network delay when deployed for ADS and SMS applications. This low delay of CAFBR in ADS applications is due to its high reliability demand compared to SMS applications. This is due to its highly reliable designed routing architecture to convey data packets from source towards destination in order to fulfil the ADS and SMS application requirements. Moreover, ineffective channel utilization and unnecessary multi-hop also leads to upsurge transmission range, which inevitably cause excessive interference in SCR, which results in extremely low network throughput for both ADS and SMS applications compared to CAFBR as shown in Fig. 4. On the other hand, the secondary channel utilization in CAFBR is found more effective compared to SCR routing scheme as shown in Fig. 5. This effective SU channel utilization leading in CAFBR leading to high network throughput and avoids corrupted data packets for both ADS and SMS applications. The residual energy profile of both routing schemes in both ADS and SMS scenarios in smart grid deployment is also shown in Fig. 6. The residual energy profile found in CAFBR is more significant than SCR routing scheme. Herein, it is noticed that the residual energy profile of CAFBR is more effective for ADS applications compared to SMS application. On the other hand, the residual energy profile in SCR is found superior for SMS than ADS applications. In sum, for both ADS and SMS scenarios, the performance of CAFBR is observed remarkable than SCR routing scheme. The low residual energy profile in SCR is because the nodes with lower battery power are used to convey data packets and due to cessation of the batteries intermediate nodes in the route it results in frequent route failures leading to a significant amount of energy consumption from source to sink. Moreover, to discover effective routes excessive message retransmission is needed which consumes a significant amount of node and neighbors energy in the network. Which is found more for SMS than ADS applications in the SCR. In our scheme CAFBR, DCA and FBR mechanisms play important

roles to keep high network residual energy and low network delay by providing a robust and link reliability aware multi-hop greedy routing architecture in the smart grid network. Which makes it extremely suitable for both ADS and SMS applications. In CAFBR, DCA channel assignment algorithm helps to assign high data capacity-aware channel between each set of pair of nodes in order to provide real-time high data rate for ADS applications in a robust manner. In DCA a longer idle channel is assigned to nodes for their reliable communication in both ADS and SMS applications. As, the longer idle probability reduces the collisions occurs between PUs and SUs and saves a significant amount of retransmission power, which is consumed during re-sensing the spectrum holes as shown in Fig. 5. To increase the channel selection reliability throughout the sensing process channel information table is periodically updated in the light of new information when deployed for both ADS and SMS applications. Furthermore, due to its unique characteristics of the restricted channel sensing mechanism helps multiple secondary users to sense desired data capacity channel in different regions simultaneously without generating excessive interference in the smart grid. In the FBR routing scheme, link quality is measured based on minimum distance information between each set of node pairs from the source towards the destination when deployed for ADS and SMS applications. The designed FBR routing architecture is responsible to distribute energy load evenly in the network by appointing a set of nodes as backbone nodes by considering their residual energy, minimum distance and angle information. Thus, it takes the advantage of shortest path routing by considering minimum and maximum d_{th} values in the network which prevents unnecessary multi-hop, data path looping and maintains residual energy profile when deployed for ADS and SMS applications. Note that, in fishbone routing network total of five fishbone independent architectures are formed on the positive axis by considering angle information between $15^{\circ}-22^{\circ}$, $51^{\circ}-58^{\circ}$, $87^{\circ}-94^{\circ}$, $123^{\circ}-130^{\circ}$ and $158^{\circ}-165^{\circ}$. The rib nodes connected to each backbone network have angle information as $350^{\circ}-280^{\circ} \leq \varphi_{sni} \leq 80^{\circ}-20^{\circ}$, $170^{\circ}-110^{\circ} \leq \varphi_{sni} \leq 80^{\circ}-20^{\circ}$ and $240^{\circ}-170^{\circ} \leq \varphi_{sni} \leq 140^{\circ}-50^{\circ}$. Also, note that the delay performance of CAFBR for SMS is observed lower than ADS applications. However, the designed scheme fully satisfies the QoS requirements for both SMS and ADS applications. Consequently, after receiving information each backbone node looks in its own routing table and select the next hop node with the minimum transmission distance. In term of a backbone route failure, routing table helps to find an appropriate next hop relay node with energy consumption to convey data packets. Here, it is important to note that to find an appropriate next hop node first sender will looks into its low transmission single hop routing table (maximum up to 10 hops neighboring nodes in range with transmission power ($30 \leq d_{th} \leq 70$) meters) if fail to find then it route information using high transmission single hop routing table information (it stored maximum up to 6 hops neighboring nodes in range with transmission power ($30 \geq d_{th} \geq 70$) meters) in the network. Thus, in sum each node is responsible to maintain dual information in its routing table called low level single hop and high-level single hop routing information differentiated by a unique pointer. This mechanism reduces the impact of management complexity at extremely low cost as a result high throughput is reported for both ADS and SMS applications in a harsh nature smart grid. Furthermore, as stated before, since this process extremely reduces the impact of data path looping and unnecessary multi-hop data transmission in both ADS and SMS applications. Therefore, the impact of control message overheads is reduced indirectly and a significant amount of network energy is saved to prolong the network lifetime of CAFBR scheme compared to SCR in both ADS and SMS applications deployment scenarios.

5. Conclusion and future work

Recent field tests show that wireless links in smart grid environments have higher packet error rates and variable link capacity because of dynamic topology changes, obstructions, electromagnetic interference, equipment noise, multipath effects, and fading. To overcome these communication challenges, in this paper, we propose a data capacity-aware channel assignment (DCA) and fish bone routing (FBR) algorithms for real-time critical, e.g., automated demand supply (ADS) and smart metering system (SMS) applications. The proposed DCA framework deals with the channel scarcities by dynamically switching between different spectrum bands and employs a network for organizing WSN into a highly stable connected hierarchy when deployed for ADS and SMS applications. In addition, the proposed FBR mechanism provides robust loop free data paths and avoids high transmission cost, excessive end-to-end delay and restricts unnecessary multi-hop data transmission from the source to destination in ADS and SMS scenarios. Thus, it significantly reduces the probability of data packet loss and preserves stable link qualities among sensor nodes for load balancing and prolonging the lifetime of WSN-based ADS and SMS applications. Comparative performance evaluations show that our proposed schemes outperform the existing communication architectures in terms of data packet delivery, communication delay and energy consumption and suitable for ADS and SMS smart grid applications. Experimental evaluation of the proposed protocols in WSN testbeds is an important future research direction.

Acknowledgements

This study was supported by the Turkish National Academy of Sciences Distinguished Young Scientist Award Program (TUBA-GEBIP) under Grant No. V.G./TUBA-GEBIP/2013-14.

References

[1] V.C. Gungor, D. Sahin, T. Kocak, S. Ergut, C. Buccella, C. Cecati, et al., A survey on smart grid potential applications and communication requirements, IEEE Trans. Ind. Inform. 9 (2013) 28–42.
[2] V.C. Gungor, B. Lu, G.P. Hancke, Opportunities and challenges of wireless sensor networks in smart grid, IEEE Trans. Ind. Electron. 57 (2010) 3557–3564.
[3] Z. Fan, P. Kulkarni, S. Gormus, C. Efthymiou, G. Kalogridis, M. Sooriyabandara, et al., Smart grid communications: overview of research challenges, solutions, and standardization activities, IEEE Commun. Surv. Tutor. 15 (2013) 21–38.
[4] J. Gao, Y. Xiao, J. Liu, W. Liang, C.P. Chen, A survey of communication/networking in smart grids, Future Gener. Comput. Syst. 28 (2012) 391–404.
[5] C. Eris, M. Saimler, V.C. Gungor, E. Fadel, I.F. Akyildiz, Lifetime analysis of wireless sensor nodes in different smart grid environments, Wirel. Netw. 20 (2014) 2053–2062.
[6] M. Yigit, O.D. Incel, V.C. Gungor, On the interdependency between multi-channel scheduling and tree-based routing for WSNs in smart grid environments, Comput. Netw. 65 (2014) 1–20.
[7] A. Ahmad, N. Javaid, S.H. Ahmed, S.H. Bouk, M. Ilahi, D. Kim, COME: cost optimisation with multi-chaining for energy efficient communication in wireless sensor networks, Int. J. Ad Hoc Ubiquitous Comput. 20 (2015) 186–198.
[8] S.H. Ahmed, D. Kim, S.H. Bouk, N. Javaid, Error control based energy minimization for cooperative communication in WSN, ACM SIGAPP Appl. Comput. Rev. 14 (2014) 55–64.
[9] A.N. Alvi, S.H. Bouk, S.H. Ahmed, M.A. Yaqub, N. Javaid, D. Kim, Enhanced TDMA based MAC protocol for adaptive data control in wireless sensor networks, J. Commun. Netw. 17 (2015) 247–255.
[10] A. Mehmood, S. Khan, D. Zhang, J. Lloret, S.H. Ahmed, Iotec: Iot based efficient clustering protocol for wireless sensor network, in: Proceedings of the International Industrial Information Systems Conference, Chiang Mai, Thailandpp, 2014, pp. 21–24.
[11] M. Faheem, M.Z. Abbas, G. Tuna, V.C. Gungor, EDHRP: energy efficient event driven hybrid routing protocol for densely deployed wireless sensor networks, J. Netw. Comput. Appl. 58 (2015) 309–326.
[12] M. Faheem, G. Tuna, V.C. Gungor, LRP: link quality-aware queue-based spectral clustering routing protocol for underwater acoustic sensor networks, Int. J. Commun. Syst. (2016).
[13] M. Basharat, W. Ejaz, S.H. Ahmed, Securing cognitive radio enabled smart grid systems against cyber attacks, in: Proceedings of the First International Conference on Anti-Cybercrime (ICACC), 2015, pp. 1–6.
[14] A.A. Khan, M.H. Rehmani, M. Reisslein, Cognitive radio for smart grids: survey of architectures, spectrum sensing mechanisms, and networking protocols, IEEE Commun. Surv. Tutor. 18 (2016) 860–898.
[15] M. Erol-Kantarci, H.T. Mouftah, Wireless sensor networks for cost-efficient residential energy management in the smart grid, IEEE Trans. Smart Grid 2 (2011) 314–325.
[16] X. Deng, L. He, X. Li, Q. Liu, L. Cai, Z. Chen, A reliable QoS-aware routing scheme

for neighbor area network in smart grid, Peer-to-Peer Netw. Appl. (2015) 1–12.
[17] H. Farooq, L. Tang Jung, Energy, traffic load, and link quality aware Ad Hoc routing protocol for wireless sensor network based smart metering infrastructure, Int. J. Distrib. Sens. Netw. 2013 (2013).
[18] H. Farooq, L.T. Jung, Health, link quality and reputation aware routing protocol (HLR-AODV) for Wireless Sensor Network in Smart Power Grid, in: Proceedings of 2012 International Conference on Computer & Information Science (ICCIS), 2012, pp. 664–669.
[19] X. Li, Q. Liang, F.C. Lau, A maximum likelihood routing algorithm for smart grid wireless network,, EURASIP J. Wirel. Commun. Netw. 2014 (2014) 1–7.
[20] Q. Wang, F. Granelli, An improved routing algorithm for wireless path selection for the smart grid distribution network, in: Energy Conference (ENERGYCON), 2014 IEEE International, 2014, pp. 800–804.
[21] R. Hou, C. Wang, Q. Zhu, J. Li, Interference-aware QoS multicast routing for smart grid,, Ad Hoc Networks 22 (2014) 13–26.
[22] M. Xiang, W. Liu, Q. Bai, Trust-based geographical routing For smart grid communication networks, in: Proceedings of the Third International Conference on Smart Grid Communications (SmartGridComm), IEEE, 2012, pp. 704–709.
[23] E. Fadel, M. Faheem, V. Gungor, L. Nassef, N. Akkari, M. Malik, et al., Spectrum-aware bio-inspired routing in cognitive radio sensor networks for smart grid applications, Comput. Commun. (2016).
[24] Y. Rong, Z. Chaorui, Z. Xing, Z. Liang, Y. Kun, Hybrid spectrum access in cognitive-radio-based smart-grid communications systems, IEEE Syst. J. 8 (2014) 577–587.
[25] R. Umar, A.U. Sheikh, A comparative study of spectrum awareness techniques for cognitive radio oriented wireless networks, Phys. Commun. 9 (2013) 148–170.
[26] ⟨http://www.estinet.com/⟩.
[27] G.A. Shah, O.B. Akan, Spectrum-aware cluster-based routing for cognitive radio sensor networks, in: Proceedings of 2013 IEEE International Conference on Communications (ICC), 2013, pp. 2885–2889.

Muhammad Faheem received the B.Sc. Computer Engineering degree in 2010 from the Department of Computer Engineering at the University College of Engineering & Technology, Bahauddin Zakariya University Multan, Pakistan. In 2012, he received an MS degree in Computer Science from the Faculty of Computer Science and Information System at Universiti Teknologi Malaysia. Currently, he is a Ph.D. student at Abdullah Gul University, Kayseri, Turkey. His research interest includes the areas of Routing in Wireless ad-hoc and Cognitive Radio Sensor Network.

Vehbi Cagri Gungor received his B.S. and M.S. degrees in Electrical and Electronics Engineering from Middle East Technical University, Ankara, Turkey, in 2001 and 2003, respectively. He received his Ph.D. degree in electrical and computer engineering from the Broadband and Wireless Networking Laboratory, Georgia Institute of Technology, Atlanta, GA, USA, in 2007. Currently, he is an Associate Professor and Chair of Computer Engineering Department, Abdullah Gul University (AGU), Kayseri, Turkey. His current research interests are in smart grid communications, machine-to-machine communications, next-generation wireless networks, wireless ad hoc and sensor networks, cognitive radio networks. Dr. Gungor has authored more than 50 papers in refereed journals and international conference proceedings, and has been serving as an Associate Editor in prestigious journals, such as for IEEE Transactions on Industrial Electronics and Ad Hoc Networks (Elsevier). He is also the recipient of the Turkish Academy of Sciences Distinguished Young Scientist Award (TUBA-GEBIP) in 2013, IEEE Trans. on Industrial Informatics Best Paper Award in 2012, the European Union FP7 Marie Curie IRG Award in 2009, AVEA Research Grant Award in 2013 and 2014, Turk Telekom Research Grant Awards in 2010 and 2012, and the San-Tez Project Awards supported by Alcatel-Lucent, and the Turkish Ministry of Science, Industry and Technology in 2010. Importantly, Dr. Gungor's recent paper on smart grid communications has been ranked 8th in the Top Accessed Article List in the IEEE Xplore as of 2012.